Journal of Hydrology: Regional Studies 62 (2025) 102938

Contents lists available at ScienceDirect

Journal of Hydrology: Regional Studies

journal homepage: www.elsevier.com/locate/ejrh

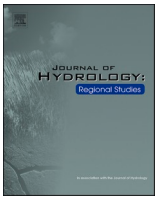

Spatiotemporal connections in high precipitation events in Iran: Application of complex networks

Mahnoor Roohinia [a], Banafsheh Zahraie [b,*]

[a] School of Civil Engineering, College of Engineering, University of Tehran, Tehran, Iran
[b] School of Civil Engineering, College of Engineering and Head of Water Institute, University of Tehran, Tehran, Iran

ARTICLE INFO

Keywords:
Complex Network
Event Synchronization
Event Coincidence Analysis
Teleconnection
High Precipitation Events
Iran

ABSTRACT

Study region: A relatively large area covering east and west Asia, north Africa, and Europe.
Study focus: This study examines the complex correlation patterns of high precipitation events in Iran and the rest of the study region. For this purpose, the Complex Networks Theory is used to find the links between high precipitation events in Iran and the rest of the study area with different time lags. The work pinpoints persistent teleconnection routes as well as changes in these routes, possibly due to global warming. Monthly GPCP precipitation values from 1980 to 2019 are used in the analysis. Precipitation events exceeding the 70th percentile in each grid cell are identified and analyzed across twenty-one annual sliding windows. The sliding windows detect the effects of global climate change on the teleconnections of high precipitation events with different lag times. Event Synchronization (ES) and Event Coincidence Analysis (EC) are utilized as complementary methods for creating adjacency matrices. Network structures are also delineated through clustering coefficient as well as betweenness centrality measures.
New hydrological insights for the region: The results of this study demonstrate that with a zero-time lag, large-scale local precipitation clusters develop synchronously over both eastern and western Iran. In contrast, when including a 2–3-month delay, precipitation clustering becomes dominant in southeast Iran. Moreover, the betweenness centrality analysis indicates a shift in critical moisture transition nodes. These nodes move from synchronous regions in southeast Iran and its border with Pakistan toward delayed routes passing through northwest Iran, southern India, and the Yemen–Saudi Arabian border. The combination of ES and lagged EC offers a dual approach for identifying both synchronous and lagged precipitation teleconnections, thereby providing a robust opportunity for the seasonal forecasting of high-precipitation events. Identifying zones with high clustering and centrality across multiple temporal scales yields new insights for developing effective early flood warning systems and effective mid-term water resources planning and management.

1. Introduction

High precipitation events in arid and semi-arid regions such as Iran can result in flash floods, land degradation, and infrastructure and crop land destruction (Katiraie-Boroujerdy et al., 2013). Even a short intense rain in dry regions may overwhelm drainage infrastructure and increase rapid runoff, enhancing the risk of flooding (Khansalari et al., 2021). Climate change has also exacerbated

* Corresponding author.
E-mail addresses: mahnoor.roohinia@ut.ac.ir (M. Roohinia), bzahraie@ut.ac.ir (B. Zahraie).

https://doi.org/10.1016/j.ejrh.2025.102938
Received 23 July 2025; Received in revised form 29 October 2025; Accepted 10 November 2025
Available online 18 November 2025

these problems by changing precipitation regimes and increasing the frequency and intensity of extreme events and Iran has not been an exception (Afsari et al., 2024). Climate change not only has affected water supply systems but also has complicated forecasting and management of flood events.

High-precipitation events often exhibit long-range teleconnections, meaning precipitation anomalies in one region can significantly influence processes in distant areas. For a country like Iran, understanding these spatial relationships is critical for improving prediction reliability, guiding early warning systems, and enabling anticipatory water resource management. By accounting for both localized and tele-connected processes, researchers can achieve a more integral understanding of high-precipitation events. This, in turn, fosters enhanced preparedness and risk mitigation against flooding.

Significant impacts of climate change on Iran and the neighboring countries in the past and projections of the probable impacts in the future have been previously studied by many researchers. The recent study by Babaeian et al. (2023) using CMIP6 climate models confirms that the nation is currently undergoing an undeniable shift in its precipitation regime. Fakour et al. (2025) used ECMWF-ERA5 reanalysis precipitation data during 1941–2020 and detected a significant shift towards more intense and more frequent high precipitation events in northwest Iran linked to global climate change. Using extreme precipitation indices developed by the Expert Team on Climate Change Detection and Indices (ETCCDI), Fattahi et al. (2025) investigated the spatiotemporal patterns of extreme rainfall at 38 synoptic stations across Iran (1990–2020). They found that all extreme indices experienced significant shifts, primarily during 2000–2010. Mahbod and Rafiee (2021) and Chaparinia et al. (2025) studied the 1992–2022 period and reported a contrasting declining trend in the frequency of extreme events (above the 90th and 95th percentiles) in northern and western regions of Iran, particularly along the Caspian Sea shoreline.

Despite all the projections related to increasing trends of extreme precipitation events in most climatological stations in Iran, available reports and research publications often suggest countrywide increasing dryness trends associate with global climate change. As an example of the recent studies, Ghazi et al. (2025) provided projections based on CMIP6 models suggesting that percent of the areas covered by BW (arid desert) and BS (semi-arid steppe) climate categories as classified by Köppen-Geigerdespite will increase in Iran by the end of the century. The results necessitate better policies for managing and capturing flood surface runoff, which is critical for mitigating the escalating water scarcity nationwide.

Over recent years, Complex Networks theory has proved effective in analyzing interrelations among climate indices (Tsonis et al., 2006) and in identifying spatial correlations of climate variables (Yamasaki et al., 2008; Donges et al., 2009). One of the strong points of complex networks is that they are not only able to represent direct relations between distinct regions but also can represent concrete paths through which teleconnections propagate (Zhou et al., 2015). By using sliding windows, changing patterns of temporal variability are tracked and assessed relative to dynamic complex networks (Radebach et al., 2013; Boers et al., 2015b). Considering the complex statistical properties of precipitation, studies making use of complex networks have been focused primarily on synchronizations of strong and extreme precipitation episodes, sometimes using event synchronization as a surrogacy measure of similarity (Malik et al., 2012; Boers et al., 2013; Boers et al., 2015a; Rheinwalt et al., 2016).

Researchers have used different methods for constructing climate networks, of which one of the most common, Event Synchronization (ES), has been used in many applications. Although widespread in its applications, this approach, in its classic mode, only deals with what happens simultaneously and ignores any possible time gap between events.

There have been a few studies in which climate networks were used to assess spatiotemporal variations and links between extreme precipitation events. Thomas et al. (2024) combined multifractal analysis and climate networks to analyze patterns of synchronization among extreme events on multiple time scales. They demonstrated that climate networks based on ES were able to capture and analyze patterns of concurrent occurrences of extreme rain events in various spatial and temporal contexts. Vallejo-Bernal et al. (2023) used complex network methods in conjunction with ES analysis to determine instances of strong rain across North America, revealing that intense atmospheric rivers triggered sequences of extreme precipitations, first along western coasts, then extending towards eastern regions following delays of up to 12 days. Similarly, Li et al. (2024) used ES-directed climate networks to identify 16 worldwide routes along which extreme rain propagates. They correlated these routes to regional weather patterns, topography, and Rossby waves' dynamics. Their analysis emphasized that their proposed methodology was able to reveal spatiotemporal rain patterns as well as precipitation predictability in Andes and Appalachian regions. Liu et al. (2024) investigated spatiotemporal evolution of monsoonal rain patterns in China's eastern regions through a complex network approach. By establishing climate networks—from ES—dissimilar connectivity patterns among rain regions were revealed, dictated by dynamic atmospheric interactions on a large scale. Their findings emphasized the ability of network methods to reveal monsoonal precipitations generation mechanisms as well as interregional linkages.

In summary, these studies confirmed that ES is a powerful tool for locating and analyzing patterns of propagation as well as synchronization of extreme rain occurrences in various regions. Contrary to this, Event Coincidence (EC) analysis can be used to assess coincidence between events, like ES but offering a more holistic consideration of time delays. Although being highly useful, there are relatively few works on its utilization in constructing precipitation networks. Donges et al. (2016) examined statistical relationships between various events using EC. The authors analyzed the temporal and spatial correlations between flood events and other related events, creating models to study and predict the behavior of complex natural systems. Their research highlighted the benefits of applying EC in non-stationary environments, its relevance in analyzing the cumulative impacts of climate variability, and anthropogenic changes to ecological as well as societal systems globally. Wolf et al. (2021) offered a comparative evaluation of ES and EC in developing functional networks from occurrences of heavy rain in South America. Both methods were applied using equivalent time delays, operating in similar conditions to enable a fair comparison of spatial-temporal network configurations. The results suggested that the adapted ES model was better suited to describe immediate versus extended synchrony, while EC was more successful in outlining propagation paths of rain occurrences due to its ability to account for time delays. ES was therefore found to be more useful in

analyzing synchrony without delay, while EC was found to be a better approach to study time-delayed relations in rain networks.

Several researchers have investigated variability in rainfall throughout Iran, but they have mostly focused on statistical associations or large-scale weather regimes alone. They have not taken into account how high rainfall events are interlinked throughout time in Iran. Previous studies hardly ever addressed how extreme rainfall events throughout dry regions such as Iran and its neighboring countries are interlinked in both time and space, or how interlinkages are affected by climate change. Also, complex networks, especially in the time-delayed mode, have not been used to find links between high precipitation events in Iran and its surrounding areas. To address these gaps, this work investigates interlinkages of Iran's heavy rainfall events with surrounding regions during the past four decades. Concretely, this work will learn (i) how heavy rainfall events throughout Iran, as a dry region, are related to such events in the rest of the study region, (ii) how interlinkages differ for events that occur concurrently and events that are lagged, and (iii) how climate change has affected interlinkages throughout time.

This study utilizes ES (EC) to find simultaneous (lagged) interlinked high rainfall months in Iran and the rest of the study area. Using ES and EC together allows for a better understanding of high precipitation behavior, showing both local patterns and teleconnections. Combining these two methods over a large area that includes Iran, its neighboring countries and extends to Europe and east Asia makes this study different than similar previously published studies. The proposed approach gives new information about how high rainfall months are connected over time and space and provides valuable information for early warning systems and seasonal water resources operation and management.

2. Study area and datasets

2.1. Study area

Geographically, Iran is in the southwest Asia between latitudes 25.06° and 38.47° N and longitudes 44.03° and 63.33° E. The country is bordered by three major bodies of water: The Caspian Sea in the north, and the Persian Gulf and the Gulf of Oman in the south. These aquatic bodies are major determiners of the climate of extensive areas of Iran, mostly by influencing evaporation processes and the transport of moisture.

The prevailing climatic conditions in Iran are mostly arid and semi-arid, with an average annual precipitation of about 250 mm. There is, however, considerable climatic diversity. For instance, average annual precipitation is characterized by extreme variations, ranging from 55 to 1355 mm in different parts of the country. Regions bordering the Caspian Sea, as well as the north and northwestern parts of Iran, tend to have greater amounts of precipitation on average. On the contrary, the southern, eastern, and central desert regions receive the lowest annual amounts of precipitation (Ashraf et al., 2014). The interactions between localized climatic processes and general atmospheric systems show the dynamics involved in the precipitation processes and considerable diversity of seasonal patterns of rainfall across Iran (Javari, 2016).

The area covered in this study is within the dashed lines shown in Fig. 1.a. This region is selected because it is assumed that most systems affecting precipitation patterns in Iran are also influential on the precipitation variations in some areas in the selected region. The map of Iran's provinces is also shown in Fig. 1.b.

From west, the study area includes the Mediterranean region because the Mediterranean precipitation system is one of the main

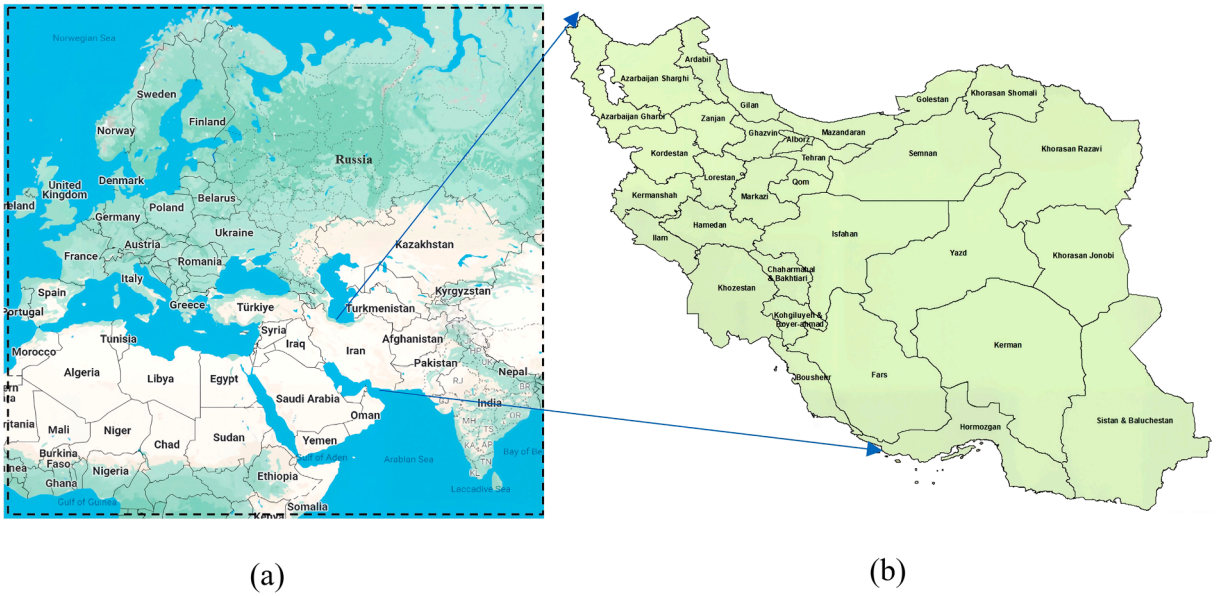

Fig. 1. (a) Study area and (b) Provinces of Iran.

sources of precipitation in the western and central parts of Iran. This system is important in maintaining the regional hydrological balance and has significant impacts on the hydrological state of extensive areas in the west, northwest and southwest of Iran during all seasons (Pourasghar et al., 2012; Heydarizad et al., 2018).

Precipitation in northern Iran is mainly controlled by frontal systems and by sea breezes on the northeast coastal part of the Caspian Sea (Shestakova and Toropov, 2021). Monsoon systems originated over India and Indian ocean cause floodings in southeast of Iran. Therefore, the eastern side of the study area is extended to include Indian subcontinent and India ocean. Floodings in southwest of Iran are also influenced by synoptic systems over Red sea and Sudan (Mohammadi et al., 2022) and systems over Saudi Arabia Peninsula are also linked to high precipitation events in south of Iran. Therefore, the study area is extended from southwest to cover Red sea and Sudan and from south to cover Saudi Arabia Peninsula.

2.2. Datasets

The Global Precipitation Climatology Project (GPCP) dataset with spatial resolution of 2.5° × 2.5°, which merges ground and satellite observations to create trustworthy global precipitation estimates, is used as the source of monthly precipitation in the present study. GPCP data was utilized in this work due to the following reasons:

- GPCP contains land and ocean, which is extremely useful in this work and permits investigating the pattern shaped both over sea and land.
- According to some studies, GPCP dataset is a reliable source of data when assessing seasonal precipitation patterns and for seasonal and monthly climate studies and analyses (Masoodian & Keikhosravi Kiany, 2014).

We also examined other datasets, but given that the study area is relatively large, working with higher resolution datasets was computationally challenging. Therefore, the moderate spatial resolution of GPCP (2.5° × 2.5°) offered us a practical balance between capturing essential precipitation patterns and maintaining computational feasibility, making it the most suitable dataset for the temporal and spatial scale of this study.

We used GPCP data in the period of 1980–2019 and selected the 70th percentile to determine high rain events. The reason for choosing the 70th percentile in this study was that at higher percentages such as 90 %, which is also frequently used in similar studies, very few links could be detected and it was not possible to assess the temporal changes in the links due to climate change.

3. Methodology

Fig. 2 shows a flowchart summarizing the study process. First, satellite-based precipitation data for the years 1980–2019 for the study area shown in Fig. 1.a were downloaded. To improve the results, data points with a mean annual precipitation of below 80 mm, which represent very arid regions, were omitted. In this study, 21 different 20-year sliding windows were considered to examine the spatiotemporal stability of links between high precipitation events. For each one of the 21 sliding windows -(1980–1999),

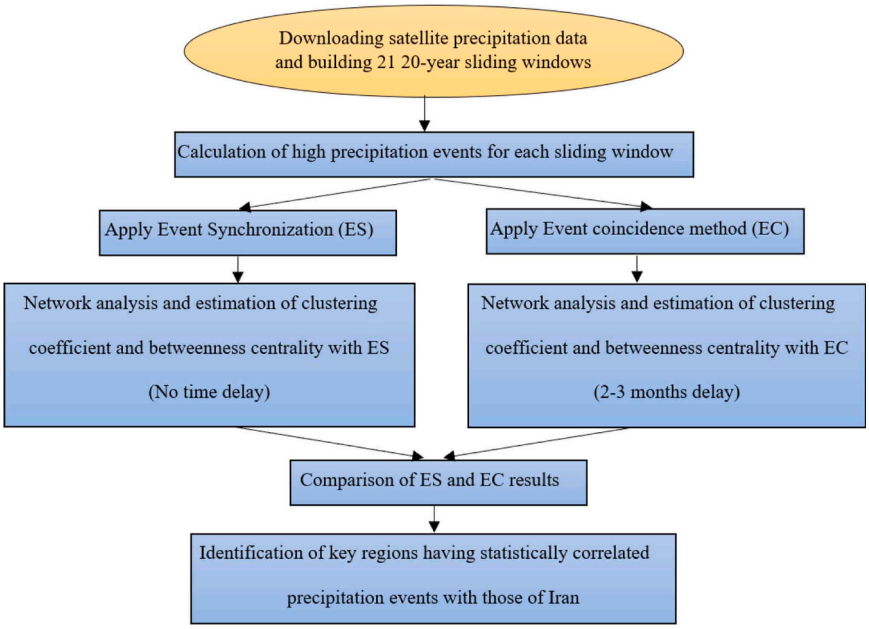

Fig. 2. Flowchart of this study.

(1981–2000), (1982–2001), …, (2000–2019)- high precipitation events were identified, then a network was created, and the ES and EC analyses were performed to examine temporal relationships between high precipitation events. In the ES approach, network analysis was performed to estimate clustering coefficients and betweenness centrality without considering any time delay, whereas in the EC approach, the same analysis was conducted with a time delay of 2–3 months. Subsequently, the results obtained from the ES and EC methods were compared. Finally, key network areas for Iran and areas that had meaningful connections (between high precipitation events) with Iran were identified. A description of the various methods and criteria used in the proposed methodology is provided in the next sections.

3.1. Concept of Event Synchronization (ES)

ES is a non-linear measure used to assess correlations between time series characterized by events (Quiroga et al., 2002; Malik et al., 2012; Agarwal et al., 2017). As mentioned in the previous section, the 70th percentile was considered in this study, to define high precipitation events.

Consider event l ($l = 1, 2, \ldots, s_i$) occurs at time t in cell i (t_l^i) and event m ($m = 1, 2, \ldots, s_j$) happens at time t in cell j (t_m^j). s_i and s_j refer to the total number of events that have taken place in cells i and j, respectively. Eq. (1) can be used to compute the minimum temporal difference between two consecutive events in cells i and j (Wolf et al., 2020):

$$\tau_{lm}^{ij} = \min\left\{ t_{l+1}^i - t_l^i \quad .t_l^i - t_{l-1}^i . t_{m+1}^j - t_m^j \quad .t_m^j - t_{m-1}^j \right\} \Big/ 2 \tag{1}$$

Here the total number of synchronized events with which the event in cell j happens after one in cell i has taken place is computed ($c(i|j)$).The parameter J_{ij}, as described in Eqs. (2) and (3), represents the number of occurrences of an event happening first in cell i before manifesting in cell j:

$$c(i|j) = \sum_{l=1}^{s_i} \sum_{m=1}^{s_j} J_{ij} \tag{2}$$

To avoid counting repeating events in a given time interval, all event pairs are weighted as per the following methodology. It is worth noting that the dynamical coincidence interval τ_{lm}^{ij} can also be bound from above, referred to as τ_{max}, which is set to one month in the no-lag time scenario.

$$J_{ij} = \begin{cases} 1 if 0 < t_l^i - t_m^j < \tau_{lm}^{ij} \\ \frac{1}{2} if t_l^i = t_m^j \\ 0. otherwise \end{cases} \tag{3}$$

The synchronization strength of events (Q_{ij}) between the cells i and j is calculated using Eq. (4):

$$Q_{ij} = \frac{c(i|j) + c(j|i)}{\sqrt{s_i s_j}} \tag{4}$$

These calculated values are then normalized to the range of 0–1. The value of 1 in Q_{ij} implies that there is ideal synchronization between two cells while that of 0 in Q_{ij} implies the non-existence of synchronization between cells. After synchronization strength normalization among different cells, the next step involves the construction of a complex network. Any two cells are connected by a link when normalized strength of synchronization is greater or equal to the predetermined threshold. According to the threshold value defined, the adjacency matrix is constructed according to Eq. (5) where Q_{ij}^0 is the threshold value which is 70 % in this study. The resulting matrix is known as the adjacency matrix (A_{ij}):

$$A_{ij} = \begin{cases} 1. if Q_{ij} \geq Q_{ij}^0 \\ 0. otherwise \end{cases} \tag{5}$$

In the ES, one of the main aims is to ensure exact synchronization in event timings in order to keep delays to the bare minimum. Basic ES systems operate based on predetermined protocols of handling temporal synchronization, thus ensuring that the event happens almost concurrently or with very minimal delay. These delays are dynamic between two events and are limited by an upper bound. On the other hand, in the EC model, the perception of synchronized events is possible by considering constant delays. In this model, events with gaps in between can still be classified as synchronized or nearly simultaneous. The main difference between ES and EC is based on how one views time delays. ES is defined by the existence of local, dynamic time intervals that quantify the temporal closeness between successive, related events. In Fig. 3a schematic illustration of ES is shown. EC uses global, fixed time interval known as ΔT that may lead to a temporal gap between two concurrent events (τ) that are classified as synchronized. Although it is possible to apply a time gap in event synchronization, in general, this gap does not exist in its formula. However, this time gap is one of the main parameters in the EC method. (Wolf et al., 2020).

3.2. Concept of Event Coincidence (EC)

Similar to the ES, assume event l ($l = 1, 2, \ldots, s_i$) occurs at time t in cell i and event m ($m = 1, 2, \ldots, s_j$) happens at time t in cell j. s_i and s_j refer to the total number of events that have taken place in cells i and j, respectively. EC analysis refers to the evaluation of coincidental occurrences across different types of events. The hypothesis in question maintains that events of type j happen before those of type i and that there may be the causal effect that occurrences of type j cause occurrences of type i. Additionally, by swapping the labels of both types i and j, the case where occurrences of category i occur before occurrences of category j can also be examined (Wolf and Donner, 2021).

A lagged coincidence is detected if the time-delayed event $t_l^i - \tau$ with $\tau \geq 0$ (as the variable representing temporal lag) and the event t_m^j satisfy the following condition:

$$(t_l^i - \tau) - t_m^j \leq \Delta T \tag{7}$$

It should be noted that the analysis of EC can also be done using coincidence intervals which are symmetric with respect to i-events, thus avoiding the requirement that j-events must precede the occurrence of i-events. The discussion that follows introduces the concept of the coincidence rate regarding one specific pair of event series.

To estimate the strength of statistical relationships between two time-significant types of occurrences, termed i and j, we define two different types of coincidence rates that group j-type occurrences as antecedents or facilitators of occurrences of type i. Eq. (8) gives precursor coincidence rate (Siegmund, 2018):

$$r_p(\Delta T.\tau) = \frac{1}{s_i} \sum_{i=1}^{s_i} \Theta \left[\sum_{j=1}^{s_j} 1_{[0.\Delta T]}\left((t_l^i - \tau) - t_m^j\right) \right] \tag{8}$$

This measure quantifies the fraction of i-type events that are preceded by at least one j-type event. Here, $\Theta(\cdot)$ shows the Heaviside function (here defined as $\Theta(x) = 0$ for $x \leq 0$ and $\Theta(x) = 1$ otherwise) and $1_{I(x)}$ the indicator function of the interval I (defined as $1_{I(x)} = 1$ for $x \in I$ and $1_{I(x)} = 0$ otherwise). The Heaviside function $\Theta(\cdot)$ is used to avoid duplicate counts of events. Eq. (9) gives the trigger coincidence rate:

$$r_t(\Delta T.\tau) = \frac{1}{s_j} \sum_{j=1}^{s_j} \Theta \left[\sum_{i=1}^{s_i} 1_{[0.\Delta T]}\left((t_l^i - \tau) - t_m^j \quad \right) \right] \tag{9}$$

This measure quantifies the fraction of j-type events that are followed by at least one resulting i-type event. Distinguishing between the coincidence of precursor and trigger resulting event series allows one to integrate in the coincidence analysis framework an essential idea of directionality. Also, the parameter τ allows one to model lagged dependencies between event series with considerable accuracy. In this method, similar to the ES method, a threshold is used to construct an adjacency matrix and complex network, which, like the previous method, is assumed to be 70 %. In Fig. 4a schematic illustration of EC is shown. In this study, the values of τ and ΔT are considered to be 2 and 1 month, respectively. The selection of a 2–3-month lag period is based on empirical observation. The first strong teleconnection links affecting precipitation in Iran consistently appeared at this delay in the initial sliding window analysis (using a threshold of 0.7). Maintaining this lag allows for a focused investigation into the dynamics of moisture transport and the timing of rainfall patterns across the country. This selection is further supported by Pakdaman et al. (2024) also endorsed this selection.

3.3. Network measurement

Any complex network has inherent topological characteristics defining its connectivity and doubtlessly its processes dynamics going on it. Thus, network analysis, break-down, and merging are based on network indicators capable of revealing its most usual

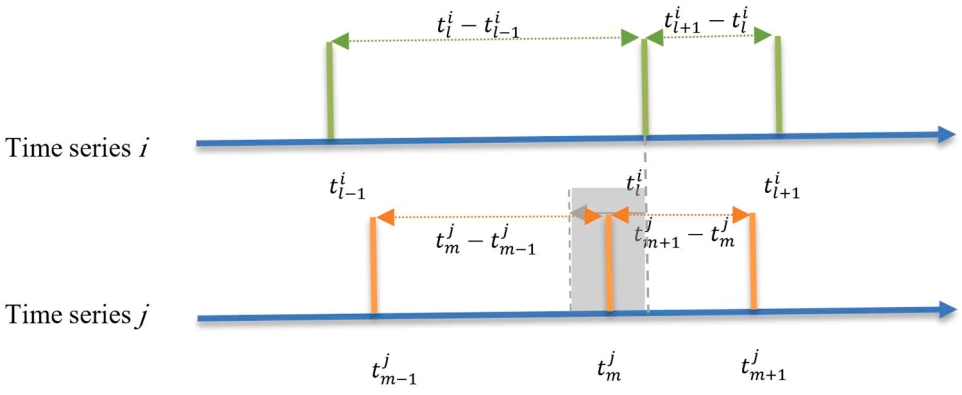

Fig. 3. A schematic illustration of ES.

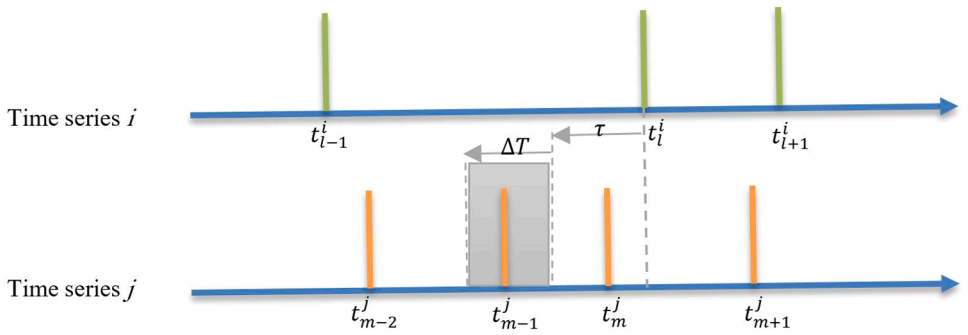

Fig. 4. A schematic illustration of EC.

properties. Numerous metrics have been proposed to examine network characteristics. Following the related previous studies, this research is focused on calculating clustering coefficient and betweenness centrality as two of the most fundamental measures in network analysis (Boers et al., 2013; Jha and Sivakumar, 2017; Deepthiand Sivakumar, 2022; Singhal et al., 2023).

The clustering coefficient (CC_j) for grid j represents the probability that two grid points connected to each other are also connected to a third grid point. In graph theory, this concept describes the extent to which the neighbors of a node approximate a complete graph, which is a graph in which all nodes are interconnected, also known as a clique.

Suppose that grid point j has k_j links, meaning it is connected to k_j other nodes. If these other nodes is also interconnected, the total number of possible links among them is given by $\frac{k_j(k_j-1)}{2}$. If the actual number of existing links is L_j, the clustering coefficient can be expressed as:

$$CC_j = \frac{2L_j}{k_j(k_j-1)} \tag{10}$$

The clustering coefficient of CCj lies between zero and one. If no neighbor of node j's is interconnected, then $CCj = 0$. If $CCj = 1$, then node j's all neighbor nodes, forming a complete graph, are interconnected. For scenarios in which clustering coefficient lies between zero and one, CCj is a probability that two neighbors of a node are interconnected. If $CCj = 0.5$, for example, there is a 50 % chance that two neighbors of any chosen node are interconnected. To define betweenness centrality, the definitions of path and shortest path in the context of a network should be first explained. A path may be defined as a series of steps through the links that comprise the network. The length of a path is in turn defined by the number of links that it includes. The shortest path between two nodes, labeled as i and j, is defined as the path that includes the minimum number of links. This minimum path is often described as the distance between nodes i and j. It is essential to note that there may be several minimum paths of the same length between any two nodes (Pósfai and Barabasi, 2016). Therefore, betweenness centrality may be defined as the sum of the proportion of the total number of minimum paths that cross through a particular grid point and the number of minimum paths between the same pair of nodes:

$$BC = \sum_{j \neq s \neq t \in V} \frac{\sigma_j(l.m)}{\sigma(l.m)} \tag{11}$$

In Equation (11), $\sigma_j\ (l,\ m)$ is the number of shortest paths between l and m that pass through j. Physically, BC represents the information paths

4. Results

4.1. ES Results

The ES method evaluates simultaneous as well as synchronous precipitation variations in several areas ignoring time lags and gaps. The use of this method is based on its capability in creating a network that allows precipitation interdependence in various areas to be evaluated.

The results of the current study suggest important variations in the clustering coefficient in various regions of Iran. In central provinces such as Isfahan and Fars, an important drop in the clustering coefficient in the consecutive sliding windows is found over time, indicating weaker network interactions and loss of precipitation pattern stability in these regions. This drop is presumably associated with climatic change as well as the decrease in synchronous precipitation occurrences in these provinces. The northern region of Iran has also experienced decrease in clustering coefficient values (Fig. 5).

In contrast, Khorasan Razavi and Khorasan Shomali Provinces in northeast of Iran and western Iran had limited changes in the clustering coefficient, indicating relative stability in precipitation patterns and network interactions in these areas. In these regions, low variability and temporal stability of the clustering coefficient indicate the continuity and persistence of precipitation spatial patterns and the conservation of correlation structures among neighboring precipitation points. The stability could also reflect the absence of serious climatic changes in atmospheric circulation patterns during the study period. Such structural stability in the

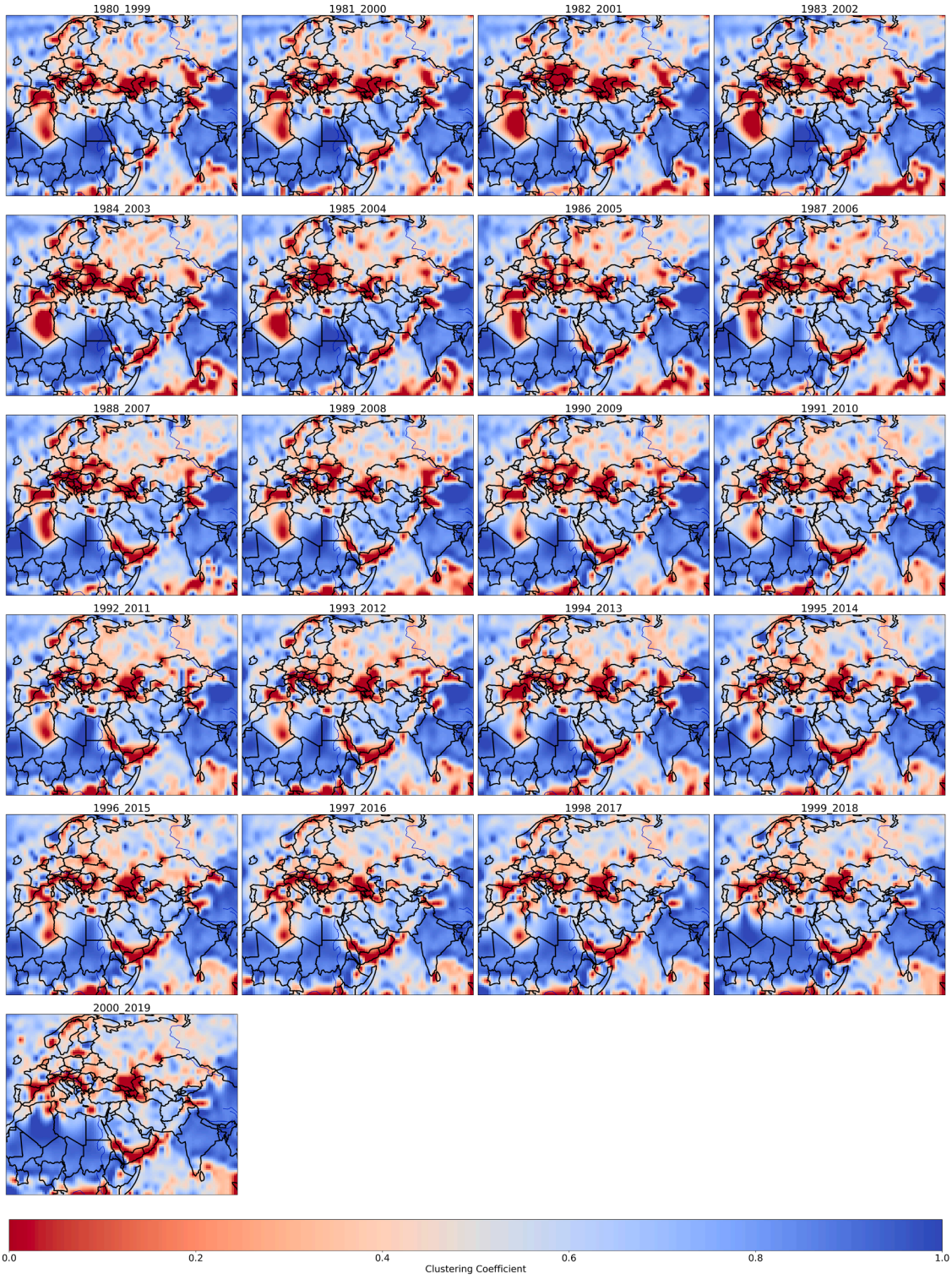

Fig. 5. Clustering coefficient for 21 sliding windows in the no-lag time scenario.

precipitation network makes precipitation behavior more predictable over the long term (Fig. 5).

In the analysis of the betweenness centrality of Iran's network of precipitation, major alterations were observed in the role of various points of precipitation over the passage of time. On the initial maps, regions such as Sistan & Baluchestan Province in southeast have had large betweenness centrality presenting consistent connectedness of precipitation.

The areas, predominantly in eastern Iran, played key roles in the network of precipitation and remained consistent over time. In the recent maps, alterations in betweenness centrality were observed in numerous regions of Iran. Particularly, Khuzestan province in southwest, which had an immense impact in the network of precipitation, presented a sharp fall in the betweenness centrality index. This can be associated with high levels of direct and indirect (climate change) human impacts Nevertheless, Sistan & Baluchestan

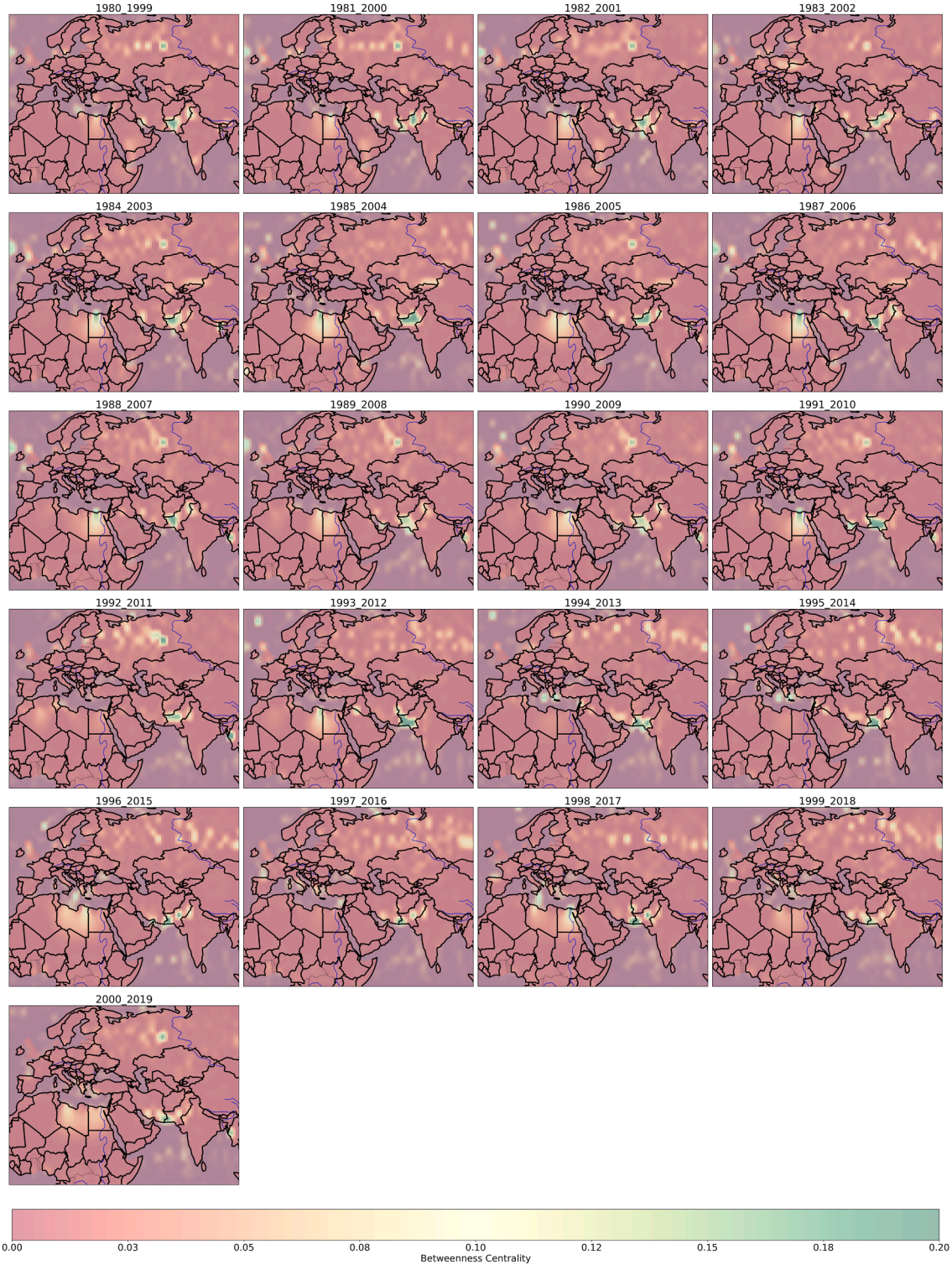

Fig. 6. Betweenness centrality for 21 sliding windows in the no-time-delay scenario.

Province in southeast has remained as a region with large betweenness centrality, with its network links remaining consistent over time (Fig. 6).

Betweenness centrality patterns reflect the extent to which various regions can be intermediaries in the regional precipitation network. Near the eastern border of Iran, the region of Pakistan registers consistently high betweenness centrality, presumably serving as a conduit for monsoon moisture to southeastern Iran; therefore, a weakening or abrupt change in this region's precipitation pattern can significantly disrupt the precipitation connectivity of Iran. Accordingly, some areas around the Mediterranean region demonstrate variability in betweenness centrality, reflecting that they can possibly impact the precipitation pattern in west of Iran, but the strength and temporal consistency can be variable over time (Fig. 6).

The persistent precipitation connections among all 21 sliding windows with no time delay are demonstrated in Fig. 7. These connections depict similar and consistent patterns of high precipitation events in Iran with those in other parts of the study area. Fig. 8 depicts two maps of major patterns of precipitation before and after 2000. Fig. 8.a depicts patterns existing prior to 2000 disappearing after the year 2000. They demonstrate how synchronized high precipitation events before 2000 disappeared possibly due to climate change or shifts in the atmospheric regimes. Fig. 8.b depicts patterns that were not present before 2000 but emerged later. It is worth mentioning that the year 2000 was selected based on the previous studies indicating significant

hydroclimatic shifts in Iran around this year. As Mansouri Daneshvar et al. (2019) stated within 138-year records, the warmest years in Iran have occurred since 2000.

4.2. EC results

This section examines the patterns of precipitation in Iran and surrounding regions by measuring events that are associated with one another after a 2–3-month delay. Contrasted with the ES method that examines precipitation patterns occurring simultaneously, this method examines how the timing of high precipitation events in a particular region can influence timing in other regions in the future and therefore, it provides an opportunity for forecasting high precipitation periods. It is worth noting that, in this study, while examining several delays, we generally concluded that a 2–3-month delay is the minimum delay at which connections can be analyzed at a threshold of 70 %.

In Iran, particularly in the recent years in the southeastern area (Sistan & Baluchestan Province), high clustering coefficient can be noticed. The high delayed clustering coefficient in the southeastern area in recent years indicates the presence of coherent spatio-temporal precipitation clusters. In the neighboring areas, the clustering coefficient in Turkey initially remained high but decreased gradually and then increased over time. These patterns exhibit climatic changes that have altered the connectivity of precipitation among regions (Fig. 9).

As shown in Fig. 10, the betweenness centrality estimated for high precipitation events with a 2–3-month time lag highlights

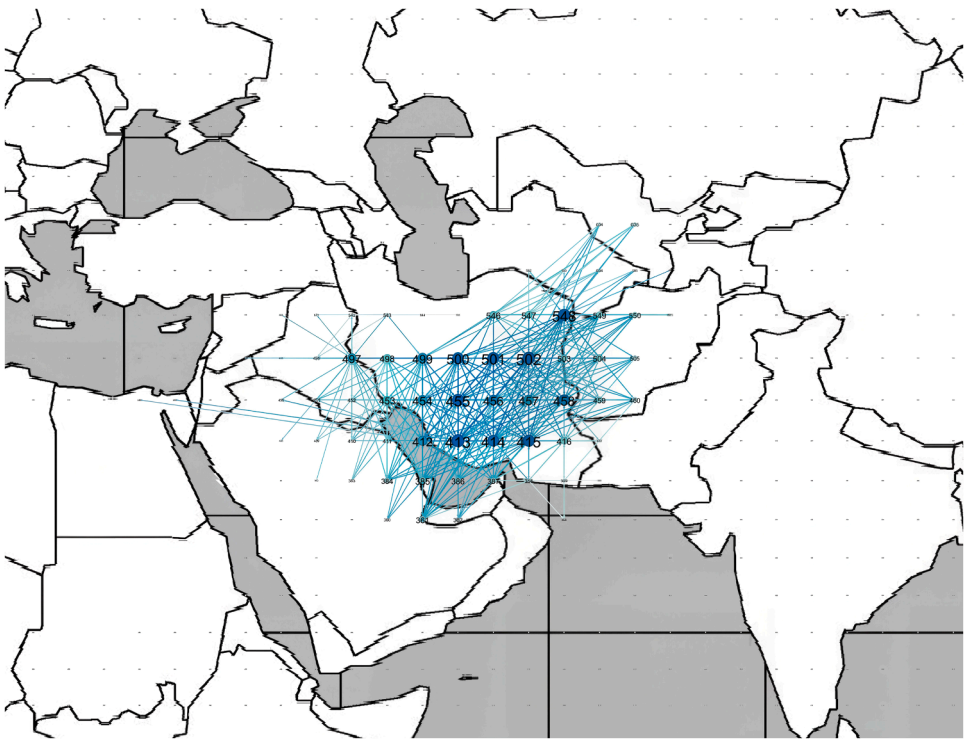

Fig. 7. Stable connections of high precipitation events in Iran in the no-lag time scenario over all sliding windows.

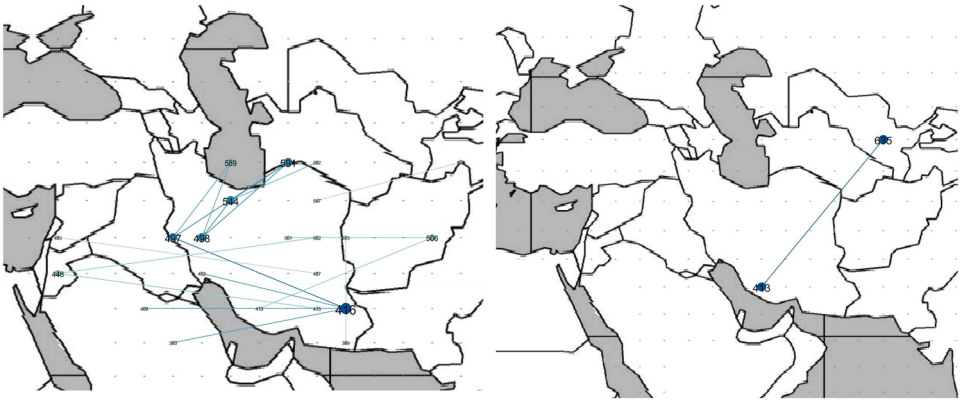

(a) (b)

Fig. 8. Comparison between (a) links that existed in all sliding windows before 2000 and disappeared afterwards and (b) links that existed only after 2000 (based on ES analysis in the no-lag time scenario).

significant changes in the precipitation network that may influence Iran. In northwestern Iran, betweenness centrality values have increased in the recent years, reflecting the growing importance of local pathways connecting precipitation clusters within the country. Additionally, southern India exhibits consistently high betweenness centrality, suggesting a possible role in transmitting delayed moisture toward Iran. Similarly, fluctuations in Saudi Arabia's betweenness centrality indicate a potential contribution to moisture transfer affecting

south and southwest of Iran. Given that high betweenness centrality in a region indicates the intermediary role of that region between different areas with various precipitation patterns, changes in the points with high betweenness centrality in the delayed scenario indicate changes in intermediary and vital points over time (Fig. 10).

The stable connections of Iran over 21 different time periods are shown in Fig. 11. These connections are associated with a 2–3-month time lag, meaning that high precipitation events in Iran occurred 2–3 months after high precipitation events occurred in outside regions shown in Fig. 11. Most of the detected connections are teleconnections spanning over thousands of kilometers. Most of the links are with India, the Indian Ocean, the North Atlantic Ocean, and the Mediterranean Sea, highlighting the significant interconnections of these regions with Iran's high precipitation periods.

Fig. 12 illustrates the changes in precipitation connections between Iran and other regions over time. In Fig. 12.a, the connections between high precipitation events in Iran and other regions that have consistently existed before the year 2000 are shown. In these connections, high precipitation events in external locations occurred 2–3 months prior to those in Iran, indicating an opportunity for long-lead forecasting. However, in Fig. 12.b, after 2000, these connections disappeared, which can be attributed to global climate changes and their impact on spatiotemporal patterns of high precipitation events.

5. Discussion

The findings of this research identified that there is a decrease in clustering coefficient of central Iran in the no-delay case, possibly reflecting disrupted synchronization of high-rainfall events because of the recent climatic variations and the growing irregularity of rainfalls. This is consistent with previous studies showing that central and southern regions of Iran have experienced decreased rainfall coherence along with increased variability (Fattahi et al., 2025). However, southeast Iran (specifically Sistan & Baluchestan Province) retained relatively higher clustering and betweenness measures. Previous studies (Khoddam et al., 2015; Mahoutchi et al., 2023) have emphasized on the influence of the monsoon systems originating from India on the precipitation of the Sistan & Baluchestan Province which can also be interpreted as the higher connectivity of high precipitation events in this part of Iran and those of India and Indian Ocean shown by the stable connections in Fig. 11. Since clustering and betweenness measures in the no lag scenario retained relatively consistent in the study period, no significant change in the near future in the synchronized precipitation events between these two regions is expected.

The high betweenness centrality values found over Saudi Arabia in the lagged case imply possible intermediary functions in the transfer of atmospheric moisture and the control of delayed precipitation over south and southwest of Iran. This result agrees with the previous studies showing probable moisture transfer from subtropical pressure belt from Saudi Arabia towards Iran (Lashkari and Mohamadi, 2015). Such teleconnections, determined on the basis of EC analysis, suggest potential for development of prediction models for high precipitation events over south of Iran with 2–3-month lead times.

Despite the robust methodological framework, a few limitations should be noted. The GPCP dataset ($2.5^\circ \times 2.5^\circ$ resolution) may not adequately capture localized precipitation variability, particularly over mountainous terrains such as the Zagros and Alborz ranges. Additionally, the 1980–2019 period, though long, may not fully encompass multi-decadal variability or extreme events beyond this window. Other drivers, such as local convective processes, Mediterranean moisture influx, or regional circulation patterns, might

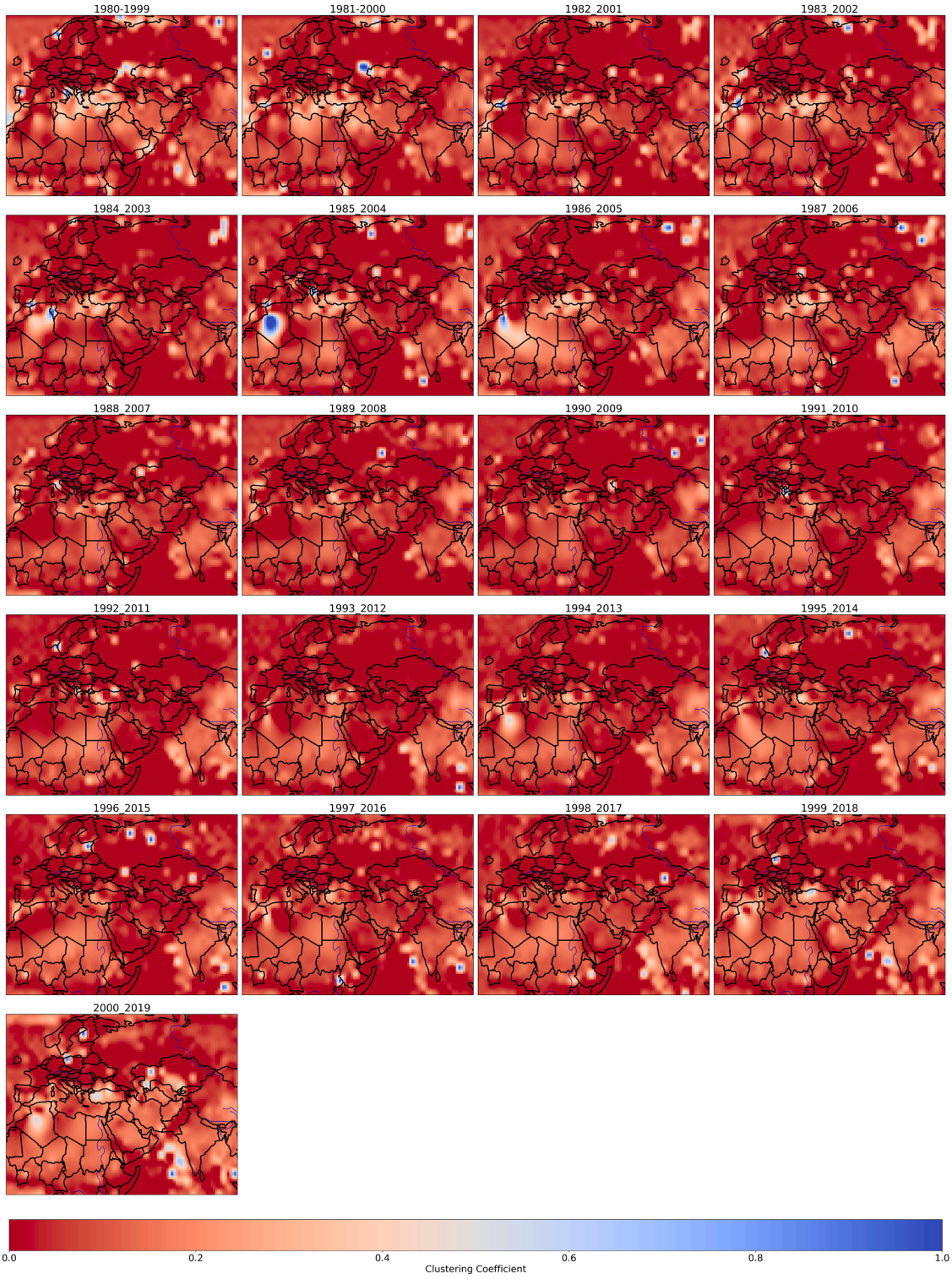

Fig. 9. Clustering coefficient for 21 sliding windows in a 2–3-month lag time scenario.

contribute to observed connections.

Some possible applications of key findings of this study are listed in Table 1 which can also be considered as subjects for future studies. Together, ES and EC synthesis provides an integrated framework for development of early warning system for high precipitation periods. This study demonstrated the relevance of methodological pluralism in climate studies and network analyses.

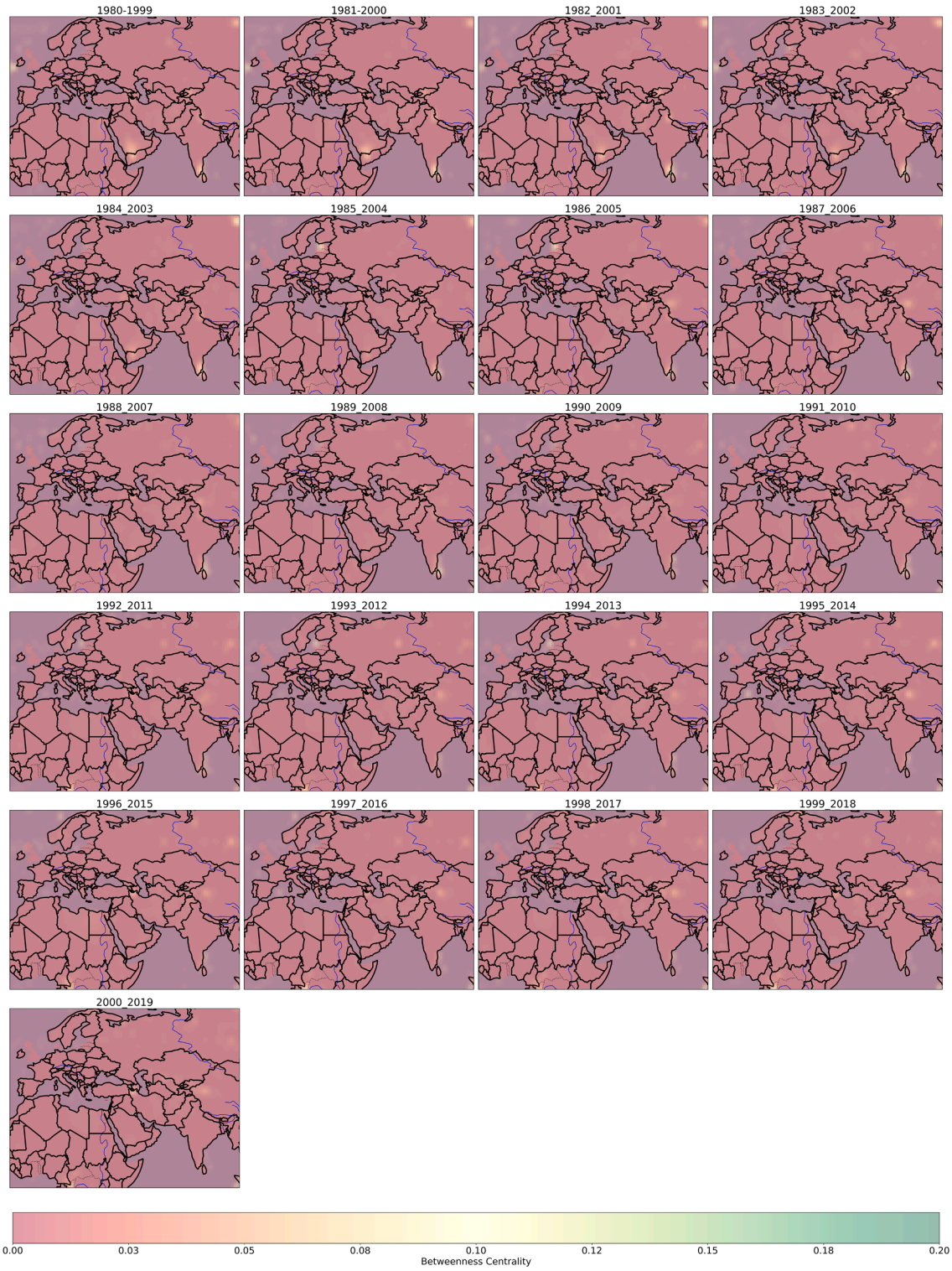

Fig. 10. Betweenness centrality for 21 sliding windows in a 2–3-month delay scenario.

6. Conclusions

This study used synchronization (ES) and event coincidence analysis (EC) to investigate the spatiotemporal relationships of high precipitation events in Iran and surrounding areas. Applying a 2–3-month lag revealed new patterns of delayed precipitation effects

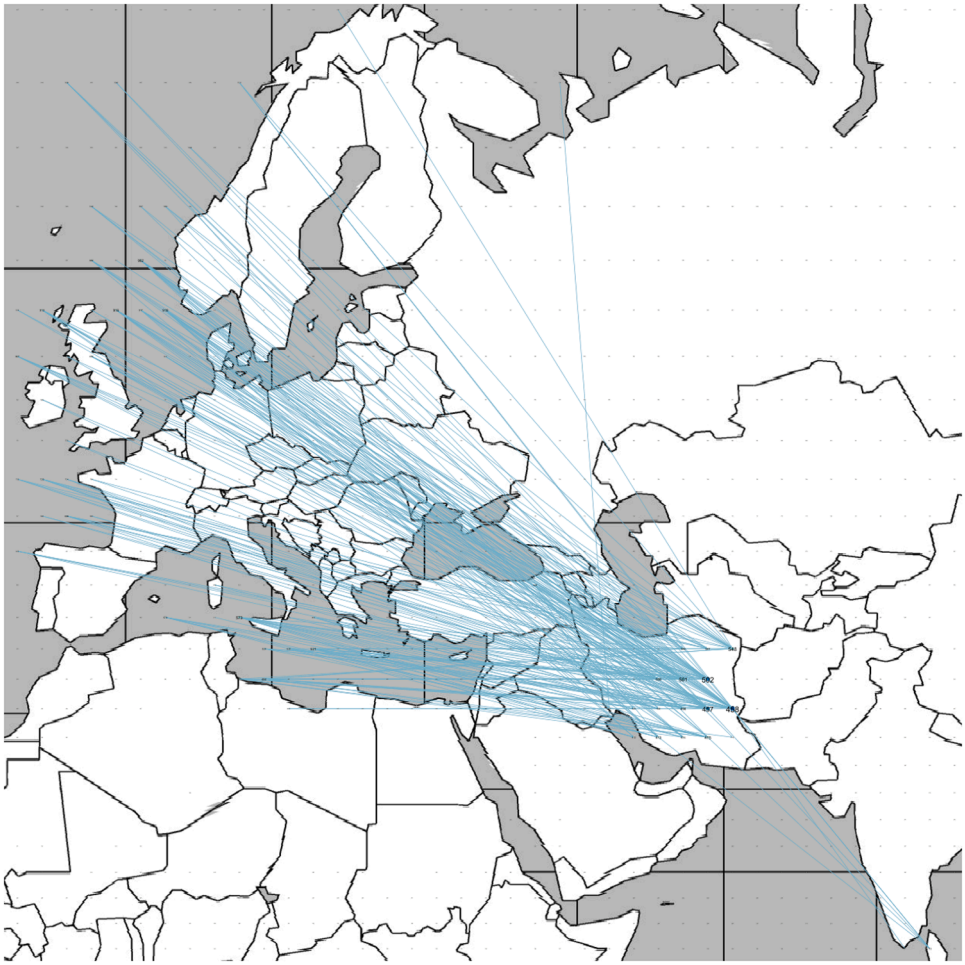

Fig. 11. Stable connections of high precipitation events in Iran in a 2–3-month time lag scenario over all sliding windows.

(a) (b)

Fig. 12. Comparison between (a) links that existed in all sliding windows before 2000 and disappeared afterwards and (b) links that existed only after 2000 (based on EC analysis in the 2–3-month lag time scenario).

that could not be detected by synchrony analysis.

Southeastern Iran often has high clustering and betweenness centrality when there is no delay, showing that it has strong local synchronization of heavy rainfall events. In the 2–3-month lag scenario, northwestern Iran, southern India, and sometimes the Yemen–Saudi Arabia border has shown high betweenness centrality. This suggests that these areas play an important role in moving

Table 1
Some applications of key regions in the precipitation network.

Region	Major findings	Possible applications of the findings
Indian Ocean & Southern India	High CC (EC) & High BC (EC)	Forecasting high precipitation months with 2–3-months lead time in southeast Iran
Turkey & Mediterranean Sea	High CC (EC)	Forecasting high precipitation months in west of Iran with 2–3-month lead time
Border of Yemen an Saudi Arabia	High BC (EC)	Forecasting high precipitation months with 2–3-month lead time in south and southwest of Iran

atmospheric moisture and affecting delayed heavy rainfall events in Iran.

The results obtained in this study provided useful implications for policymakers and the research community. Areas with high clustering coefficient and betweenness centrality in time-lagged scenarios, such as the Indian Ocean and southern India, can be suitable candidates for selecting points to predict high precipitation events in Iran with a lead time of 2–3 months. This is very important in flood prevention, risk reduction, and water resources management.

Future studies could employ higher-resolution datasets and integrate regional climate model simulations to validate and extend these network-based findings. Applying multi-scale temporal lags (e.g., seasonal or annual) and including additional climatic variables like sea surface temperature, geopotential height, or soil moisture could provide deeper insight into the mechanisms governing precipitation teleconnections. The stable connections identified here could be incorporated into predictive frameworks for flood forecasting, drought preparedness, and climate resilience planning. Strengthening these analyses with finer spatial and temporal granularity will enhance the predictive and operational value of network-based hydrological studies across arid and semi-arid regions.

CRediT authorship contribution statement

Banafsheh Zahraie: Writing – review & editing, Validation, Supervision, Formal analysis. **Mahnoor Roohinia:** Writing – original draft, Visualization, Validation, Software, Methodology, Formal analysis, Data curation, Conceptualization.

Declaration of Competing Interest

The authors declare that they have no known competing financial interests or personal relationships that could have appeared to influence the work reported in this paper.

Data Availability

Data will be made available on request.

References

Afsari, R., Nazari-Sharabian, M., Hosseini, A., Karakouzian, M., 2024. A CMIP6 Multi-Model Analysis of the Impact of Climate Change on Severe Meteorological Droughts through Multiple Drought Indices—Case Study of Iran's Metropolises. Water.16 5, 711. https://doi.org/10.3390/w16050711.
Agarwal, A., Marwan, N., Rathinasamy, M., Merz, B., Kurths, J., 2017. Multi-scale event synchronization analysis for unravelling climate processes: a wavelet-based approach. Nonlinear Process. Geophys. 24 (4), 599–611.
Ashraf, B., Yazdani, R., Mousavi-Baygi, M., Bannayan, M., 2014. Investigation of temporal and spatial climate variability and aridity of Iran. Theor. Appl. Climatol. 118, 35–46.
Babaeian, I., Modirian, R., Khazanedari, L., Karimian, M., Kouzegaran, S., Kouhi, M., Malbusi, S., 2023. Projection of Iran's precipitation in 21st Century using downscaling of selected CMIP6 Models by CMHyd. J. Earth Space Phys. 49 (2), 431–449.
Boers, N., Bookhagen, B., Marwan, N., Kurths, J., Marengo, J., 2013. Complex networks identify spatial patterns of extreme rainfall events of the South American Monsoon System. Geophys. Res. Lett. 40 (16), 4386–4392.
Boers, N., Donner, R.V., Bookhagen, B., Kurths, J., 2015. Complex network analysis helps to identify impacts of the El Niño Southern Oscillation on moisture divergence in South America. Clim. Dyn. 45, 619–632.
Boers, N., Bookhagen, B., Marengo, J., Marwan, N., von Storch, J.S., Kurths, J., 2015. Extreme rainfall of the South American monsoon system: a dataset comparison using complex networks. J. Clim. 28 (3), 1031–1056.
Chaparinia, F., Hadei, M., Yaghmaeian, K., Hadi, M., Naddafi, K., 2025. Evaluation of climate indices related to water resources in Iran over the past 3 decades. Sci. Rep. 15 (1), 11846.
Deepthi, B., Sivakumar, B., 2022. General circulation models for rainfall simulations: Performance assessment using complex networks. Atmos. Res. 278, 106333.
Donges, J.F., Zou, Y., Marwan, N., Kurths, J., 2009. The backbone of the climate network. Europhys. Lett. 87 (4), 48007.
Donges, J.F., Schleussner, C.F., Siegmund, J.F., Donner, R.V., 2016. Event coincidence analysis for quantifying statistical interrelationships between event time series: On the role of flood events as triggers of epidemic outbreaks. Eur. Phys. J. Spec. Top. 225, 471–487.
Fakour, R., Ustrnul, Z., Wypych, A., 2025. Risk assessment of extreme precipitation in northwest Iran in the light of changing climate. Int. J. Climatol. https://doi.org/10.1002/joc.8854.
Fattahi, E., Kamali, S., Asadi Oskouei, E., Habibi, M., 2025. Investigating the spatiotemporal variation in extreme precipitation indices in Iran from 1990 to 2020. Water 17 (8), 1227.
Fattahi, E., Kamali, S., Asadi Oskouei, E., Habibi, M., 2025. Investigating the spatiotemporal variation in extreme precipitation indices in Iran from 1990 to 2020. Water 17 (8), 1227.
Ghazi, B., Salehi, H., Cheshami, M., Zeydalinejad, N., Linh, N.T.T., 2025. Projection of climate change impact on main climate variables and assessment of the future of Köppen–Geiger climate classification in Iran. Acta Geophys. 73 (2), 2017–2027.
Heydarizad, M., Raeisi, E., Sori, R., Gimeno, L., Nieto, R., 2018. The role of moisture sources and climatic teleconnections in Northeastern and South-Central Iran's hydro-climatology. Water 10 (11), 1550.
Javari, M., 2016. Trend and homogeneity analysis of precipitation in Iran. Climate 4 (3), 44.
Jha, S.K., Sivakumar, B., 2017. Complex networks for rainfall modeling: Spatial connections, temporal scale, and network size. J. Hydrol. 554, 482–489.

Katiraie-Boroujerdy, P.S., Nasrollahi, N., Hsu, K.L., Sorooshian, S., 2013. Evaluation of satellite-based precipitation estimation over Iran. J. Arid Environ. 97, 205–219.
Khansalari, S., Ranjbar-Saadatabadi, A., Fazel-Rastgar, F., Raziei, T., 2021. Synoptic and dynamic analysis of a flash flood-inducing heavy rainfall event in arid and semi-arid central-northern Iran and its simulation using the WRF model. Dyn. Atmospheres Oceans 93, 101198.
Khoddam, N., Irannejad, P., Ahmadi-Givi, F., 2015. A study of the impact of Indian Monsoon on summer climate of Iran. Iran. J. Geophys. 9, 2.
Lashkari, H., Mohamadi, Z., 2015. The role of Saudi Arabian sub-tropical high pressure on the rainfall systems on south and southwest Iran. Phys. Geogr. Res. 47 (1), 73–90.
Li, K., Huang, Y., Liu, K., Wang, M., Cai, F., Zhang, J., Boers, N., 2024. Key propagation pathways of extreme precipitation events revealed by climate networks. npj Clim. Atmos. Sci. 7 (1), 165.
Liu, L., Gao, C., Zhu, Z., Zhang, S., Tang, X., 2024. Spatiotemporal evolution patterns and underlying formation mechanisms of monsoon rainfall across eastern China: A complex network perspective. Atmos. Res. 304, 107363.
Mahbod, M., Rafiee, M.R., 2021. Trend analysis of extreme precipitation events across Iran using percentile indices. Int. J. Climatol. 41 (2), 952–969.
Mahoutchi, M.H., Abbasi, E., Khoshakhlagh, F., Rousta, I., Olafsson, H., Baranowski, P., Krzyszczak, J., 2023. Atmospheric circulation patterns during the summertime precipitation in Southeastern Iran. Atmosphere 14 (11), 1673.
Malik, N., Bookhagen, B., Marwan, N., Kurths, J., 2012. Analysis of spatial and temporal extreme monsoonal rainfall over South Asia using complex networks. Clim. Dyn. 39, 971–987.
Mansouri Daneshvar, M.R., Ebrahimi, M., Nejadsoleymani, H., 2019. An overview of climate change in Iran: facts and statistics. Environ. Syst. Res. 8 (1), 1–10.
Masoodian, A., Keikhosravi Kiany, M.S., 2014. Introduction and a Comparison among Gridded Precipitation Database of Asfazari with GPCC, GPCP and CMAP. Geogr. Res. (10174125) 29 (1).
Mohammadi, F., Pazhoh, F., Hombari, F.J., 2022. Sudan low changes affecting rainy days in southwestern Iran over six decades (1957–2019). J. Water Clim. Change 13 (2), 1056–1072. https://doi.org/10.2166/wcc.2021.311.
Pakdaman, M., Fattahi, E., Javanshiri, Z., 2024. Forecasting the average monthly rainfall in the northwest of Iran using teleconnections and machine learning. Iran. J. Geophys. 18 (2), 77–90.
Pósfai, M., Barabasi, A.L., 2016. Network Science. Cambridge University Press, Cambridge, UK. ⟨https://assets.cambridge.org/97811070/76266/frontmatter/9781107076266_frontmatter.pdf⟩.
Pourasghar, F., Tozuka, T., Jahanbakhsh, S., Sari Sarraf, B., Ghaemi, H., Yamagata, T., 2012. The interannual precipitation variability in the southern part of Iran as linked to large-scale climate modes. Clim. Dyn. 39, 2329–2341.
Quiroga, R.Q., Kreuz, T., Grassberger, P., 2002. Event synchronization: a simple and fast method to measure synchronicity and time delay patterns. Phys. Rev. E 66 (4), 041904.
Radebach, A., Donner, R.V., Runge, J., Donges, J.F., Kurths, J., 2013. Disentangling different types of El Niño episodes by evolving climate network analysis. Phys. Rev. EStat. Nonlinear Soft Matter Phys. 88 (5), 052807.
Rheinwalt, A., Boers, N., Marwan, N., Kurths, J., Hoffmann, P., Gerstengarbe, F.W., Werner, P., 2016. Non-linear time series analysis of precipitation events using regional climate networks for Germany. Clim. Dyn. 46, 1065–1074.
Shestakova, A.A., Toropov, P.A., 2021. Orographic and lake effect on extreme precipitation on the Iranian coast of the Caspian Sea: a case study. Meteorol. Atmos. Phys. 133, 69–84.
Siegmund, J.F., 2018. Quantifying Impacts Clim. Extrem. Events Veg. Event coincidence Anal. Appl. Across Scales (Dr. Diss. Univ. Potsdam). ⟨https://publishup.uni-potsdam.de/files/40709/siegmund_diss.pdf⟩.
Singhal, A., Jaseem, M., Jha, S.K., 2023. Spatial connections in extreme precipitation events obtained from NWP forecasts: A complex network approach. Atmos. Res. 282, 106538.
Thomas, A.J., Kurths, J., Schertzer, D., 2024. Multifractality of Climate Networks. EGUsphere 2024, 1–12.
Tsonis, A.A., Swanson, K.L., Roebber, P.J., 2006. What do networks have to do with climate? Bull. Am. Meteorol. Soc. 87 (5), 585–596.
Vallejo-Bernal, S.M., Wolf, F., Boers, N., Traxl, D., Marwan, N., Kurths, J., 2023. The role of atmospheric rivers in the distribution of heavy precipitation events over North America. Hydrol. Earth Syst. Sci. 27 (14), 2645–2660.
Wolf, F., Donner, R.V., 2021. Spatial organization of connectivity in functional climate networks describing event synchrony of heavy precipitation. Eur. Phys. J. Spec. Top. 230 (14), 3045–3063.
Wolf, F., Bauer, J., Boers, N., Donner, R.V., 2020. Event synchrony measures for functional climate network analysis: a case study on South American rainfall dynamics. Chaos Interdisciplinary Journal Nonlinear Science 30 (3).
Yamasaki, K., Gozolchiani, A., Havlin, S., 2008. Climate networks around the globe are significantly affected by El Nino. Phys. Rev. Lett. 100 (22), 228501.
Zhou, D., Gozolchiani, A., Ashkenazy, Y., Havlin, S., 2015. Teleconnection paths via climate network direct link detection. Phys. Rev. Lett. 115 (26), 268501.